iomac
International Operational Modal Analysis Conference
11th International Operational Modal Analysis Conference
20 - 23 May 2025 | Rennes, France

Harmonic removal for Automated Operational Modal Analysis of coupled rotor foundation system influenced by magnetic bearings and gas seals

Nathali Dreher[1], Mona Amer[2], Tiago Machado[3]

[1] University of Campinas, School of Mechanical Engineering, Campinas, Brazil, nathalidreher@gmail.com
[2] The University of British Columbia, Department of Civil Engineering, Vancouver, Canada, mona.amer@ubc.ca
[3] University of Campinas, School of Mechanical Engineering, Campinas, Brazil, tiagomh@fem.unicamp.br

ABSTRACT

Automated Operational Modal Analysis is recurrent for the modal identification of civil structures. However, its use for rotating machines is hampered by non-linearities, time-invariance, and overall superimposing harmonic excitation. In particular, harmonic excitation can either mask or disturb the identification of structural modes with natural frequencies close to the harmonics. Sometimes, harmonic frequencies can also be identified as modes with low damping, disturbing the modal identification of the system. The literature has already proposed harmonic removal methods, but most have only been tested on a few simple rotating systems. The idea behind this study is to evaluate a pre-processing method for harmonic removal in a complex rotating system, composed of a rotor supported by magnetic bearings and influenced by gas seals whose rotation is given by an electric motor. Data was acquired with different rotation speeds and the harmonic removal method was applied to generate clean signals. To evaluate the method's performance, AOMA was applied to the original and clean signals. Analysis reveals that the harmonic removal method was capable of both removing the harmonics and enabling the identification of physical modes previously masked by them. The modal identification was also compared to references from a mathematical model of the test rig and Experimental Modal Analysis tests. Results show that the combination of the harmonic removal method and AOMA enabled the identification of many physical modes of interest, especially the rotor mode that defines the stability margin of the system, that is, the operating point at which the system becomes unstable. Differences between the identified modal parameters and the references exist, which is expected, especially in the identification of damping ratios. These presented results are another contribution to support condition monitoring of complex rotating systems via Operational Modal Analysis.

Keywords: Automated Operational Modal Analysis, Rotating Machines, Gas Seals, Harmonic Removal Method.

1. INTRODUCTION

The first Operational Modal Analysis (OMA) approaches date back a few decades ago, with traditional methods such as Frequency Domain Decomposition (FDD) [1,2], Ibrahim Time Domain (ITD) [3], and Stochastic Subspace Identification (SSI) [4,5] being popular, although limited by the technology of the time. The growing interest in OMA methods is notable, as new methods and additional processing techniques are constantly developed. The success of such a group of techniques is given by its capability of extracting modal parameters of systems based solely on their outputs. For that, OMA techniques assume that the input of a time-invariant and linear system can be described as white noise excitation, which is valid for many existing systems. Nevertheless, an insurmountable number of systems cannot be described with such assumptions, either because they are non-linear and time-varying or because they are subjected to excitations that are only poorly approximated by white noise signals. Rotating machines, for example, are classical systems that are unsuitable for traditional OMA methods.

In its most simple definition, a rotating machine consists of elements that spin around their axis (rotors) and are supported by bearings, being able to produce rotational movement. Taking this definition into account, one can identify the first challenge for OMA's application in the presence of harmonic excitation instead of pure white noise. Moreover, rotating machines are time-varying systems in which the modal parameters vary according to the rotation because of the gyroscopic effect. Components such as bearings and seals also bring more complexity into the system, with parameters dependent on the operational point or ambient conditions. Many rotating machines also have non-linearities, either by the presence of non-linear components, such as hydrodynamic bearings, or friction that can be modeled with non-linear approaches. The conditions in which rotating machines operate, vary significantly with their application. Although many rotating machines work on locations with ambient excitation that might be described as white noise, this is not always true, and attention must be given to the excitation conditions. Rotating machines are present in the most diverse fields of engineering, being key components for the automotive, aerospace, and energy production sectors. The idea that OMA might be used for condition monitoring of such critical branches of industry motivates researchers to create solutions for the application of OMA to rotating systems.

Regarding the harmonic influences, traditional methods such as the FDD and the SSI can indicate the presence of harmonics. In the FDD method, harmonic frequencies appear as sharp peaks at the first and many of the lower singular value curves [6]. As for the SSI method, harmonics are usually identified as modes with negative damping or damping close to zero, and the stabilization diagram of the SSI method can be built in a way that these modes are identified as spurious and discarded from the following analyses. However, harmonics may appear next to modes of interest, harming or hindering their identification, and pre-processing techniques were developed to deal with these problems.

Many pre-processing methods for harmonic removal were proposed to remove harmonics before OMA is even applied. Among them, there are the Frequency Domain Editing (FDE) and Order Domain Deletion (ODD) methods to remove stationary and non-stationary harmonics from the signals. These methods were proposed in [7] and tested in signals from a simple numerical system, successfully removing the harmonics and getting modal estimates close to the references. Gres et al [8] proposed a harmonic removal method based on orthogonal projections and validated it on experimental data from an aluminum plate and a ship in operation, both with harmonics near the natural frequencies. For both cases, the method was successful in removing the harmonics and leading to more accurate modal identification. Gioia et al [9] investigated the use of the cepstrum editing technique to remove the harmonic influences from signals of a field-operational wind turbine's drivetrain. Results comparing the modal parameters identified after the harmonic removal with results from the condition, in which the harmonic influence is neglectable showed consistency in the estimates. More recently, Gua, Chen, and Wang [10] proposed a modified window function to remove the periodic excitation components with the cepstrum method, which surpassed problems with the traditional window functions, effectively reducing random disturbances and diminishing periodic components.

In this paper, a pre-processing method for harmonic removal is evaluated. The method was proposed in [11] and it uses information about the rotation displacement taken by a tachometer to remove the harmonics from the vibration signals. Signals from an operating rotor influenced by the dynamics of gas

seals were collected with different rotating frequencies and both the harmonic removal and Automatic Operational Modal Analysis (AOMA) algorithms were applied to identify the modal parameters of the system. The identified parameters are compared with references from a mathematical model, EMA results, and AOMA tests of the test rig without rotation. Difficulties in applying OMA to rotating systems due to the presence of harmonic components remain an open problem, especially in complex systems, where traditional harmonic removal techniques have not proven effective. Therefore, the present study provides valuable contributions to this field.

2. METHODOLOGY

This section presents information about the test rig and the method used for harmonic removal. Section 2.1 brings a brief description of the components and functioning of the test rig, modal results from the mathematical model, EMA, and AOMA tests. Section 2.2 presents the harmonic removal method.

2.1. Test Rig

The test rig displayed in Figure 1 is composed of a main shaft (rotor) supported by two active magnetic bearings (AMB) and influenced by two smooth annular seals. For the drive, an electric motor is used. An assembly of a drive shaft, a belt drive, and a flexible coupling connect these two components. The test rig is in a testing area at the Technical University of Denmark (DTU), which enabled a controlled environment during the tests. It is possible to operate the test rig with different seal inlet pressures and add white noise excitation into the system via the active magnetic bearings. Given the controlled environment, the two main possible sources of excitation are the turbulent gas flow within the seals and white noise from the bearings. Hall effect sensors are used to measure vibration. They are completely embedded in the pole surface areas of the two AMBs, measuring the displacement of the shaft in relation to the magnetic bearings in the x and y directions with a sampling frequency of approximately 3012 Hz. More information about the test rig's design and sensor positioning is available in [12].

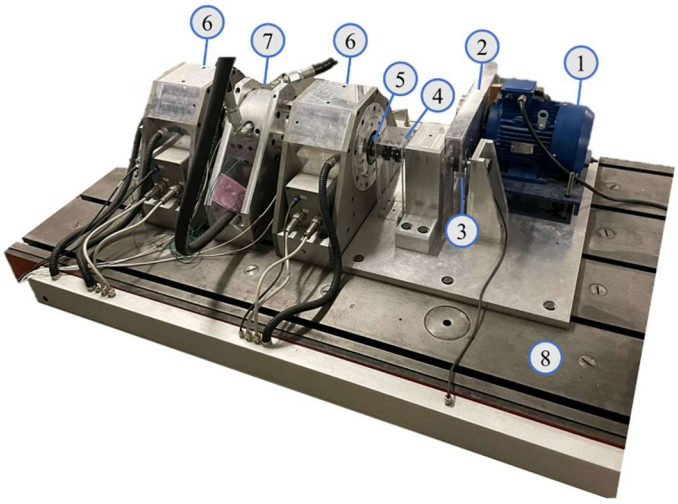

Figure 1. Test rig, composed of a motor (1), a belt drive (2), a drive shaft (3), a flexible coupling (4), a main shaft (5), two magnetic bearings (6), two smooth annular seals (7), and a bed plate (8).

2.1.1. Mathematical Model

A mathematical model of the test rig was developed and validated in [13]. The following components were used to describe the dynamics of the system: the rotor, the foundation, a pair of magnetic bearings, feedback control loops, machine feet, a mechanical flexible coupling, and seals. Modal parameters of the system were identified along pressure ranging from 0 bar to 4 bar, generating the results of Figure 2. Figure 2-a displays the damped natural frequencies while Figure 2-b displays the damping ratios of

the identified modes. In their investigation, Paulsen, Santos, and Clemmensen [13] associated the four modes in orange solid lines with the rotor movements, while the remaining modes (blue dashed lines) were associated with the coupled rotor-foundation movements. In the current research, the four modes associated with the rotor are called rotor modes, and the remaining modes are called coupled RF (Rotor-Foundation) modes. Special attention needs to be drawn to the second rotor mode of the system. In [13], this mode was found to define the stability margin of the test rig, that is, the operating pressure at which the system becomes unstable. The instability threshold of a system influenced by gas seals can be established when the negative damping effects of a mode overtake the positive damping effects [14]. As one can note, the damping ratio of this rotor mode turns negative around 3.8 bar pressure, which defines the stability margin of the system. In this research, this mode is identified with the acronym SM (Stability Margin).

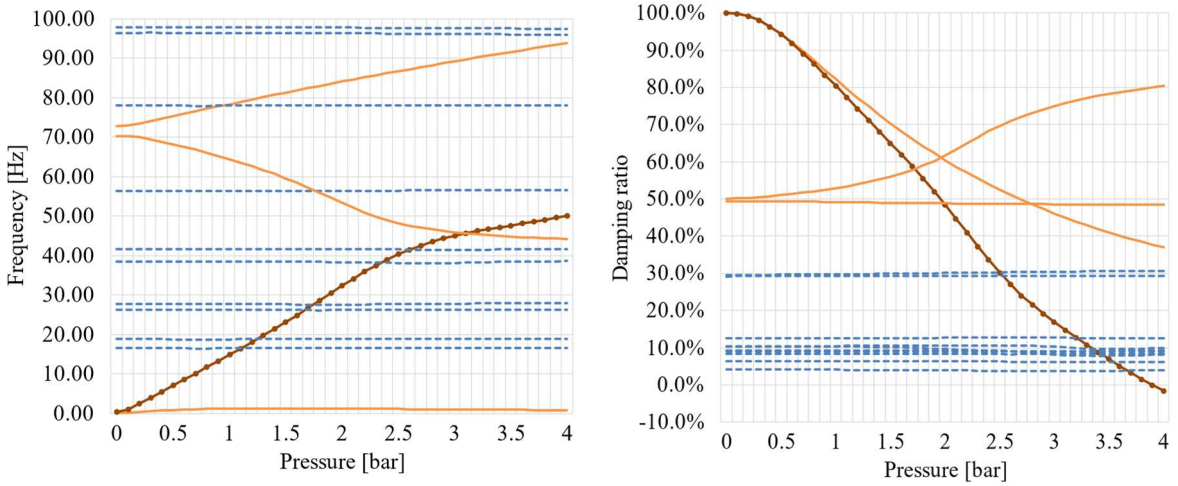

Figure 2. Damped natural frequencies (a) and damping ratios (b) from the mathematical model along different pressures, adapted from [13].

In this research, only results for 1.5 bar pressure will be analyzed. This value was arbitrarily selected to condense the results. Table 1 presents the undamped natural frequency and the damping ratio of the identified modes for 1.5 bar pressure. A column indicating to which structure the identified mode is associated was also added to Table 1. These values will be used as references for the results obtained with AOMA.

Table 1 – Results from the mathematical model for 1.5 bar and no rotation, adapted from [13].

Mode	ω_n	ζ	Source
1	1.79	70.3%	rotor
2	16.55	3.9%	coupled RF
3	18.89	9.1%	coupled RF
4	26.41	8.4%	coupled RF
5	27.78	10.1%	coupled RF
6	30.46	65.1%	rotor (SM)
7	38.60	9.3%	coupled RF
8	41.92	10.5%	coupled RF
9	56.90	12.6%	coupled RF
10	71.97	56.0%	rotor
11	78.16	6.4%	coupled RF
12	93.29	49.0%	rotor

2.1.2. *Experimental Modal Analysis*

EMA tests were also carried out to determine the modal parameters of the coupled rotor-foundation system and to have references to evaluate the OMA results [15]. For the EMA tests, the rotor was mounted in the foundation, an excitation hammer was used to excite the foundation, and acceleration measurements were collected from the bed plate. Since there were no sensors to capture the dynamics of the rotor, the EMA test captured mainly vibration patterns from the foundation. Therefore, the modes extracted from the EMA tests are identified as foundation modes in this research. Further details about the EMA tests can be found in [15], but a summary of these results is displayed in Table 2.

Table 2 – EMA results for 1.3 bar and standstill condition, adapted from [15].

Mode	ω_n [Hz]	Standard Deviation	ζ	Standard Deviation
1	24.73	0.92	8.69 %	2.54 %
2	34.71	1.28	4.00 %	2.47 %
3	42.85	0.00	13.02 %	0.00 %
4	55.94	0.37	2.08 %	1.23 %
5	73.99	0.24	1.91 %	0.65 %
6	95.10	1.30	1.55 %	1.41 %

2.1.3. *Automated Operational Modal Analysis*

AOMA was applied to vibration signals of the test rig with 1.5 bar pressure within the seals, no white noise excitation from the magnetic bearings, and no rotation. In this case, the main source of excitation is the turbulent flow within the seals. The algorithm used for AOMA was published in [16]. The parameters used to generate these results were a damping limit of 0% to 90%, a frequency variation limit of 0.5%, a damping variation limit of 4%, a MAC (Modal Assurance Criterion) limit of 90%, and a threshold limit of 0.013, which were set according to [17]. The algorithm with the additional step was applied, which guarantees that all modes within the clusters that originated the identified modes have at least 90% coherence via MAC between them. Table 3 presents the mean values and standard deviation for the undamped natural frequency (ω_n) and damping ratio (ζ) of each mode. Comparing this table with Table 1, one can see that the rotor mode that defines the stability margin is identified with 31.68% damping, which is around half the reference value from the mathematical model. Some explanations for that include inaccuracies from the mathematical model, which, although very detailed, is unable to capture all dynamics of the system, and frictional damping that might be occurring, as explained in [11]. Moreover, modes 10, 11, and 12 from the mathematical model (Table 1), and 2 and 5 from EMA (Table 2) are identified with damping values close to the reference cases.

Table 3 – AOMA Results for 1.5 bar pressure and no rotation.

ω_n [Hz]	Standard Deviation	ζ	Standard Deviation	Source
30.32	0.08	31.68%	1.64%	rotor (SM)
34.23	0.13	6.81%	6.55%	foundation
72.47	0.43	1.82%	0.63%	foundation
79.82	0.25	4.28%	0.86%	unknown
87.12	0.04	33.10%	0.11%	unknown
91.99	0.03	32.85%	0.11%	rotor
97.94	0.05	27.24%	0.63%	unknown
99.40	0.40	2.99%	0.16%	coupled RF

2.2. Methods for Harmonic Removal

The traditional cepstrum method was applied to the data, however, it was not able to remove harmonics while maintaining the modal information from the system. The spectrum and both graphical and automatic results of OMA were analyzed after the harmonic removal with cepstrum. Although the method was able to reduce harmonic influences, it did not remove them completely and ended up reducing the modal information of the signals. Therefore, another method for harmonic removal was investigated.

As mentioned in the introduction, there are different approaches to eliminate the influence of harmonics. One technique, belonging to the area of pre-processing, seeks to find a mathematical formulation for the harmonic signal component. In a second step, this harmonic signal is then subtracted from the original measured signal to obtain solely the signal part due to ambient excitation. To define the harmonic signal, a Fourier series development is used. It is aimed at finding polynomial coefficients by means of a least-squares approach that defines the Fourier series and thus the harmonic signal. The single steps to create the Fourier series can be found in [11]. It has proven successful to use the measured phase information at every time stamp if available, as it is possible to obtain better results. The harmonic removal process does not interfere with the neighboring frequency area and at the same time closely spaced structural modes with regards to the harmonics can be identified reliably.

The procedure is described in the infographic below, see Figure 3.

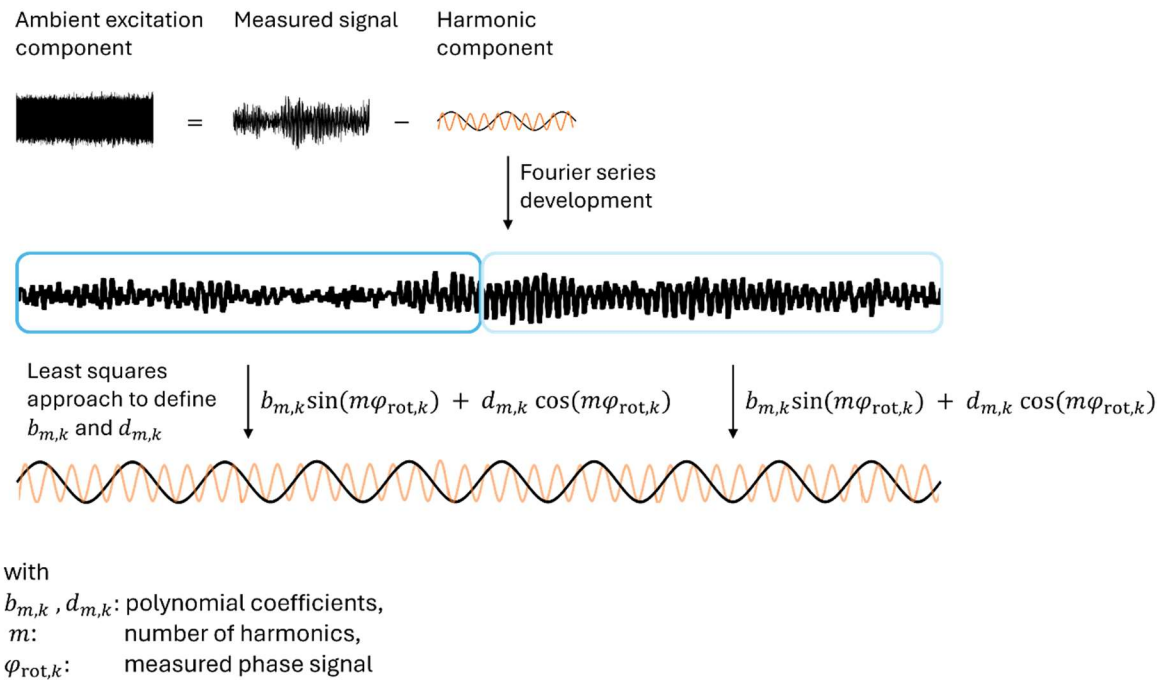

Figure 3. Process for harmonic removal based on [11].

The technique described has been applied to the data set used in this study. As described in [11], the true advantage of this technique using the measured phase information of the rotor instead of an estimated, constant frequency value for the rotation becomes clear when using large time segments of the data for the formulation of the Fourier series. A segment size of 24064 samples has been used, which equals a measurement length of 8 seconds. Different segment sizes have been tested previously, and the long dataset led to an accurate estimation of the rotor mode's damping value, which is known from the mathematical model as well as tests in standstill conditions.

3. RESULTS

Rotating speeds of 30 Hz, 45 Hz, and 60 Hz were analyzed. Due to the rotor speed control, the values of the rotor speed were almost constant at 30.92 ± 0.03 Hz, 45.60 ± 0.06 Hz, and 60.32 ± 0.10 Hz. No additional excitation from the magnetic bearings was used. Therefore, the main sources of excitation were the white noise excitation from the turbulent gas flow within the seals and unbalance forces caused by rotation. Signals in which the harmonic removal method is applied will be called *clean signals* throughout the paper.

Different segment sizes were tested for the harmonic removal method. Figure 4 displays the FDD and SSI-DATA results for the original signal (Figure 4-a), the clean signal using segments of 2048 samples (Figure 4-b), and the clean signal using segments of 24064 samples (Figure 4-c) for the rotating speed of 30 Hz. The SSI-DATA results are displayed using the stabilization diagram, in which only stable poles are displayed to facilitate the view. Comparing the FDD curves from the original signal with the ones from the clean signals, one can see that the harmonic removal method was effective, although the use of smaller segments generated valleys where the harmonics used to be, while the use of larger segments was able to smooth the FDD curves. Comparing the SSI-DATA results, the use of larger segments supports the alignments of stable poles. Further analysis showed that larger segments resulted in better estimation of modal parameters near the rotating frequency, especially the damping ratio. Thus, the following analysis will be carried out with segments of 24064 samples for the harmonic removal method.

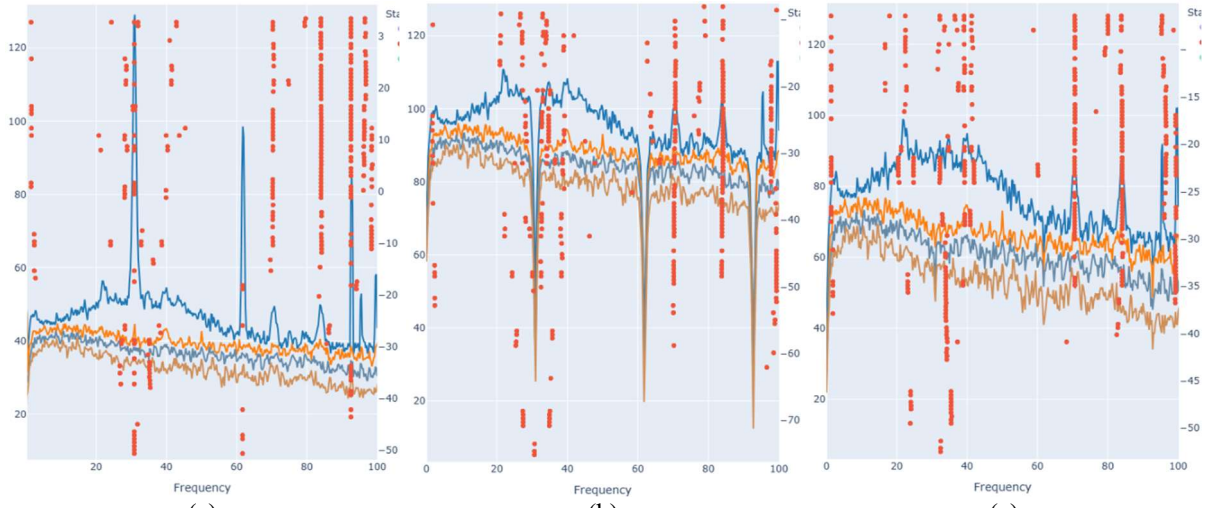

(a) (b) (c)

Figure 4. Stabilization Diagram and FDD curves for the original signal (a), the clean signal using segments of 2048 samples (b), and the clean signal using segments of 24064 samples (c), rotating speed of 30 Hz.

The Probability Density Function (PDF) of the original and clean signals were compared for the rotating speed of 30 Hz. The strong impact of the harmonics on the data can be captured when looking at the PDF resulting from the data. Whereas the PDF for the original data set containing the harmonic signal components (Figure 5-a) resembles the PDF for a harmonic function with two distinct peaks at the borders of its definition interval, the PDF after cleaning the measured data from the harmonic signal (Figure 5-b) fits the expected PDF of a Gaussian curve. This underscores the usefulness of the proposed technique as well as the strong influence of the speed-synchronous response part that can severely harm the modal identification of the system in operation.

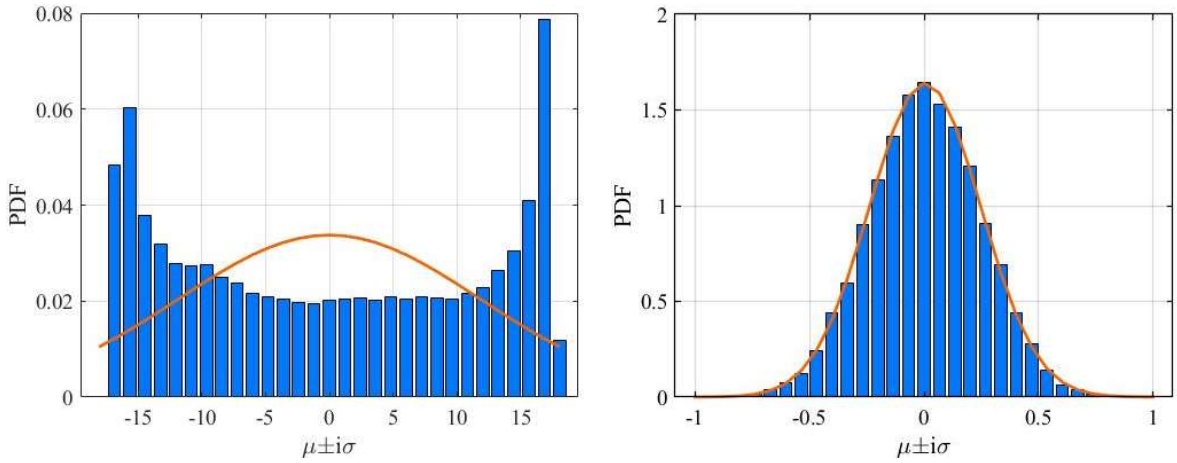

Figure 5. PDFs of the original signal (a) and clean signal (b) for the rotating speed of 30 Hz.

Table 4 presents the results of the modal identification via AOMA for the original and clean signal from the condition of 1.5 bar pressure and rotating speed of 30 Hz. Results are displayed in terms of the undamped natural frequency and damping ratio of each identified mode, alongside the standard deviation of the estimates. A column indicating the most likely source of each mode according to Table 1 and Table 2 was also added to support the analysis. From Table 4, the harmonic removal method was able to remove harmonics previously identified as physical modes (depicted in bold letters) and reveal modes once hidden, such as the one that defines the stability margin. The stability margin mode is identified with 34.01 Hz, which is around 12% higher than the same mode identified in standstill condition (Table 3). This difference can be explained by the gyroscopic effect, mainly caused by the rotor's anisotropy, which is responsible for changing the rotor's natural frequencies with rotation. The coupled RF modes are also identified with a significantly lower damping ratio when compared to the mathematical model's results (Table 1). This might be explained by inaccuracies from the mathematical model, the presence of friction damping in experimental results, or influences of other modes that are still under investigation. Modes with unknown sources were also identified by AOMA, which requires more investigation to understand if they are in fact modes of the system, coupling of different frequencies, or even spurious modes that were not properly eliminated during the AOMA analysis.

Table 4 – AOMA results for 1.5 bar pressure and rotating frequency of 30 Hz.

Original Signal				Clean signal				
ω_n [Hz]	Standard Deviation	ζ	Standard Deviation	ω_n [Hz]	Standard Deviation	ζ	Standard Deviation	Source
30.92	**0.00**	**0.00%**	**0.00%**	-	-	-	-	harmonic
-	-	-	-	34.01	0.16	37.85%	0.45%	rotor (SM)
-	-	-	-	39.29	0.05	0.49%	0.11%	coupled RF
-	-	-	-	41.32	0.14	3.89%	1.02%	coupled RF
70.46	0.02	0.88%	0.15%	70.60	0.04	0.82%	0.08%	foundation
84.23	0.03	1.00%	0.07%	84.08	0.03	1.19%	0.12%	unknown
92.75	**0.00**	**0.01%**	**0.00%**	-	-	-	-	harmonic
96.72	0.24	1.47%	0.05%	96.18	0.46	1.35%	0.25%	foundation
98.59	0.03	1.38%	0.04%	99.36	0.03	0.17%	0.10%	unknown

Table 5 presents the results of the modal identification via AOMA for the original and clean signal from the condition of 1.5 bar pressure and rotating speed of 45 Hz. In this case, the first harmonic (45.6 Hz) wasn't identified in the original signal by the AOMA method. Nevertheless, the harmonic removal method enabled the identification of modes that were hidden by the rotating frequency, including two modes from the rotor and one from the foundation. The stability margin mode was also identified with higher frequency when compared to the standstill condition results, which is again explained by the gyroscopic effect. In general, damping is identified with lower values compared to the references, which is again traced back to the friction damping and inaccuracies from the references.

Table 5 – AOMA results for 1.5 bar pressure and rotating frequency of 45 Hz.

Original Signal				Clean Signal				
ω_n [Hz]	Standard Deviation	ζ	Standard Deviation	ω_n [Hz]	Standard Deviation	ζ	Standard Deviation	Structure
-	-	-	-	1.91	0.01	61.14%	2.58%	rotor
24.63	0.10	7.68%	0.28%	24.41	0.13	7.72%	0.51%	foundation
-	-	-	-	35.19	0.13	33.51%	1.85%	rotor (SM)
-	-	-	-	49.34	0.13	2.38%	0.11%	unknown
-	-	-	-	57.89	0.02	0.54%	0.12%	foundation
-	-	-	-	61.49	0.17	2.37%	0.68%	unknown
66.30	0.24	3.41%	0.34%	66.37	0.18	3.49%	0.18%	unknown
68.62	0.11	2.06%	0.23%	68.06	0.17	3.72%	0.17%	unknown
79.18	0.08	1.27%	0.10%	79.09	0.13	1.32%	0.15%	coupled RF
91.19	**0.00**	**0.00%**	**0.00%**	-	-	-	-	harmonic
93.75	0.02	0.08%	0.02%	93.80	0.01	0.04%	0.01%	unknown
99.91	0.11	0.85%	0.06%	-	-	-	-	unknown

Table 6 presents the results of the modal identification via AOMA for the original and clean signal from the condition of 1.5 bar pressure and rotating speed of 60 Hz. The harmonic was removed with no harmful effect on the modal identification. No hidden mode was revealed, which was expected since there are no modes from the mathematical model or EMA tests close to the rotating speed of 60 Hz.

Table 6 – AOMA results for 1.5 bar pressure and rotating frequency of 60 Hz.

Original Signal				Clean Signal				
ω_n [Hz]	Standard Deviation	ζ	Standard Deviation	ω_n [Hz]	Standard Deviation	ζ	Standard Deviation	Structure
16.10	0.00	0.21%	0.02%	16.10	0.00	0.21%	0.02%	coupled RF
33.73	0.10	33.62%	1.62%	33.67	0.10	33.41%	1.71%	rotor (SM)
44.53	0.04	2.29%	0.23%	44.64	0.05	2.19%	0.11%	foundation
60.32	**0.00**	**0.00%**	**0.00%**	-	-	-	-	harmonic
75.37	0.03	0.89%	0.06%	75.41	0.08	1.00%	0.24%	foundation
90.33	0.04	0.57%	0.18%	90.31	0.03	0.52%	0.09%	unknown
91.46	0.17	1.66%	0.17%	91.33	0.34	1.68%	0.19%	unknown

The MAC between AOMA modes was computed to investigate the connection between the estimates. The MAC matrix was computed between the original signal with no rotation (Table 3) and the clean signal with a rotation of 30 Hz (Table 4) and displayed in Figure 6-a. The MAC matrix computed between the clean signals with rotation of 30 Hz (Table 4) and 45 Hz (Table 5) and displayed in Figure 6-b. The MAC value goes from 0%, indicating no coherence between two modes, to 100%, indicating complete coherence between them. From Figure 6, one can see that the highest MAC is achieved for the rotor mode defining the stability margin, being 99.8% when comparing the result with no rotation with the one with rotation of 30 Hz and 98.4% when comparing the result with rotation of 30 Hz and 45 Hz, which indicates that these modes are the same one along different measurements. There are other high values in both MAC matrices. There is 95.1% coherence between the rotor mode of 34.01 Hz and the foundation mode of 34.23 Hz (Figure 6-a), which might be explained by the influence of another rotor mode close to the foundation one. There is also 93.0% coherence between two rotor modes of 1.91 Hz and 34.01 Hz. Recalling that the data was acquired through four sensors collecting the displacement between the rotor and the two bearings, it is comprehensible that the rotor modes have high MAC values. Setting a threshold of 98% to associate identified modes with the same physical mode, which is an acceptable limit, the identification of the rotor mode defining the stability margin is validated. Moreover, the four sensors were able to capture the dynamic influence from the foundation and the coupled rotor foundation systems, identified by their natural frequencies and damping ratios. Nevertheless, they were not enough to capture their mode shapes, which explains the low MAC between the other physical modes.

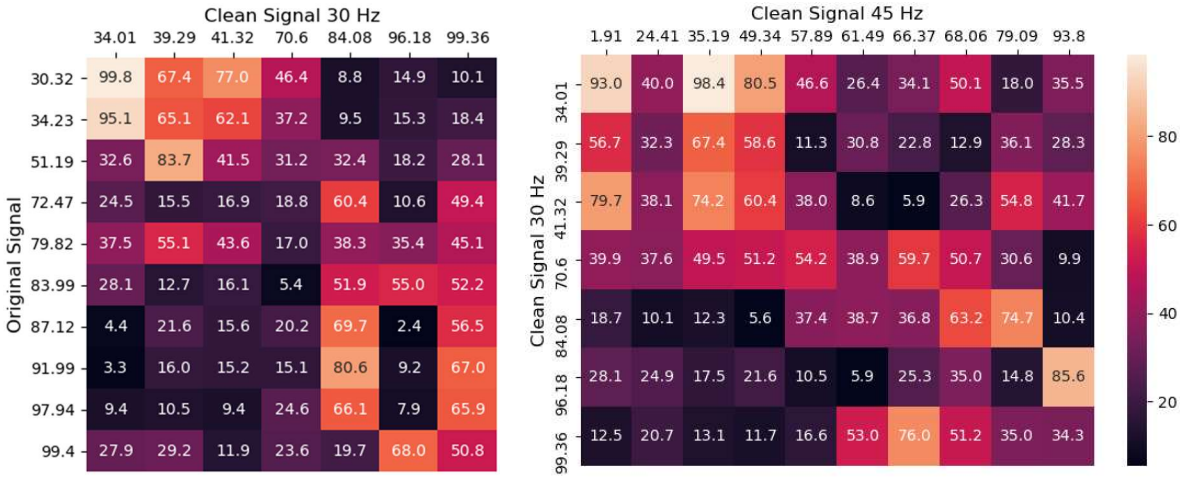

(a) (b)

Figure 6. MAC matrix between the original signal with no rotation and the clean signal of 30 Hz (a) and the clean signals of 30 Hz and 45 Hz (b).

4. CONCLUSIONS

In this paper, a pre-processing method for harmonic removal was evaluated with data from a rotor supported by magnetic bearings and influenced by gas seals. The harmonic removal was performed for different rotating speeds of the test rig, generating signals clear from the harmonics of the rotating speed. AOMA was applied and results were compared to references from EMA tests and a mathematical model of the test rig. The harmonic removal method was effective in eliminating harmonics from the rotating speed, which enabled the identification of physical modes previously masked by these harmonics. With that, AOMA was able to identify many physical modes of interest, including the rotor mode that defines the stability margin of the system. Differences in the estimates in comparison to the references were explained by the dynamic behavior of the test rig, such as the gyroscopic effect and friction damping, inaccuracies in the mathematical model, and the influence of other modes identified by the AOMA algorithm. It was possible to identify modes with high damping, in general, related to rotor dynamics. Modes that could not be identified as physical modes of the system are under investigation, alongside

results from other operating conditions and rotating frequencies. Nevertheless, it was proved that the harmonic removal method is effective and enables an accurate estimation of the physical modes of the system, being a powerful tool to support modal identification of complex rotating machines via AOMA.

ACKNOWLEDGEMENTS

The authors would like to thank CAPES, Coordination for the Improvement of Higher Education Personnel, and PRPG, Pro-Rectory of Graduate Studies at UNICAMP, for the financial support, and the Department of Civil and Mechanical Engineering from the Technical University of Denmark for providing data and support to this work.

REFERENCES

[1] R. Brincker, L. Zhang, and P. Andersen. Modal Identification from Ambient Response using Frequency Domain Decomposition. In Proc. International Modal Analysis Conference (IMAC), San Antonio, Texas, 2000.

[2] R. Brincker, C. E. Ventura, and P. Andersen. Damping Estimation by Frequency Domain Decomposition. In *Proc. International Modal Analysis Conference (IMAC): A Conference on Structural Dynamics*. Florida, USA, 2001.

[3] S. R. Ibrahim. Random Decrement Technique for Modal Identification of Structures. *Journal of Spacecraft and Rockets*, 14(11), 696-700, 1977.

[4] P. Van Overschee and B. De Moor. *Subspace Identification for Linear Systems: Theory, Implementation, Applications.* Kluwer, Dordrecht, The Netherlands, 1996.

[5] B. Peeters and G. De Roeck. Stochastic System Identification for Operational Modal Analysis: A Review. *Journal of Dynamic Systems Measurement and Control*, 123(4), 659-667, 2001. https://doi.org/10.1115/1.1410370

[6] R. Brincker and C.E. Ventura. *Introduction to Operational Modal Analysis*. 1. ed. John Wiley & Sons, Chichester, 2015.

[7] A. Brandt. A signal processing framework for operational modal analysis in time and frequency domain. *Mechanical Systems and Signal Processing*, 115, 380-393, 2019. https://doi.org/10.1016/j.ymssp.2018.06.009

[8] S. Gres, M. Döhler, P. Andersen, and L. Mevel. Kalman filter-based subspace identification for operational modal analysis under unmeasured periodic excitation. *Mechanical Systems and Signal Processing*, 146, 2021. https://doi.org/10.1016/j.ymssp.2020.106996.

[9] N. Gioia, P.J. Daems, C. Peeters, M. El-Kafafy, P. Guillaume, and J. Helsen. Influence of the Harmonics on the Modal Behavior of Wind Turbine Drivetrains. *Rotating Machinery, Vibro-Acoustics & Laser Vibrometry*, 7, 231-238, 2019. https://doi.org/10.1007/978-3-319-74693-7_22.

[10] L. Guan, Y. Chen, and Z. Wang. Operational Modal Analysis of CNC Machine Tools Based on Flank-Milled Surface Topography and Cepstrum. *Vibration*, 7, 738-763, 2024. https://doi.org/10.3390/vibration7030039

[11] M. Amer, C.E. Ventura, N. Maroldt, J.R. Seume, and J. Wallaschek. Modal parameter estimation of turbomachinery in operation taking into account friction damping. *Mechanical Systems and Signal Processing*, 216, 111414, 2024. https://doi.org/10.1016/j.ymssp.2024.111414

[12] A. J. Voigt, C. Mandrup-Poulsen, K.K. Nielsen, and I.F. Santos. Design and Calibration of a Full Scale Active Magnetic Bearing Based Test Facility for Investigating Rotordynamic Properties of Turbomachinery Seals in Multiphase Flow. *ASME. J. Eng. Gas Turbines Power*, 139(5), 052505, 2017. https://doi.org/10.1115/1.4035176.

[13] T. T. Paulsen, I.F. Santos, and L.K.H. Clemmensen. Contribution to the estimation of force coefficients of plain gas seals with high preswirl considering rotor-foundation dynamics. *Mechanical Systems and Signal Processing*, 186, 109885, 2023. https://doi.org/10.1016/j.ymssp.2022.109885.

[14] M.L. Adams, *Rotating Machinery Vibration: from analysis to troubleshooting.* Marcel Dekker Inc., Nova York, 2000.

[15] T.T. Paulsen, S.V. Damsgaard, and I.F. Santos, Automated Modal Parameter Estimation for Coupled Rotor-Foundation Systems Using Seal Forces as Excitation Source. *Mechanical Systems and Signal Processing*, 212, 111293, 2024. https://doi.org/10.1016/j.ymssp.2024.111293.

[16] N.R. Dreher, G.C. Storti, and T.H. Machado. Automated Operational Modal Analysis for Rotating Machinery Based on Clustering Techniques. *Sensors*, 23, 1665, 2023. https://doi.org/10.3390/s23031665.

[17] N.R. Dreher, T.H. Machado, T.T. Paulsen, and I.F. Santos. Identification of Modal Parameters of Coupled Rotor Foundation System via Automatic Operational Modal Analysis. In *Proc. 27th International Congress of Mechanical Engineering.* Florianopolis, Brazil, 2023.